Plasmacytoid cells in salivary pleomorphic adenoma: an alternative interpretation of their immunohistochemical characteristics highlights function and capability for epithelial–mesenchymal transition

Ioannis G. Koutlas, DDS, MS,[a] Michelle Dolan, MD,[b] Mark W. Lingen, DDS, PhD,[c] and Prokopios P. Argyris, DDS, MS, PhD[a,d]

Objectives. Plasmacytoid cells (PLCs) in salivary pleomorphic adenoma (SPA) are regarded as modified neoplastic myoepithelia and define plasmacytoid myoepithelioma (pMYO). However, histochemically, immunohistochemically and ultrastructurally, PLCs fail to demonstrate frank myogenous properties. Epithelial–mesenchymal transition (EMT) may explain the phenotypes in SPA. Our aim was to evaluate (1) PLCs with accepted or purported myoepithelial and EMT-related markers; and (2) pMYOs for *PLAG1* aberrations by using fluorescence in situ hybridization.

Study Design. Eight SPAs with or without PLC-predominance and 3 pMYOs were immunohistochemically studied.

Results. PLCs in SPA and pMYO exhibited strong, scattered to diffuse positivity for K7, rare K14 positivity and were mostly negative for α-smooth muscle actin, h-caldesmon, and p63/p40. S100 staining was strong and diffuse, whereas calponin was variable. DOG1 was negative. PLCs in pMYO and PLC-rich SPA exhibited selective or diffuse WT1 and D2-40 immunoreactivity. EMT markers SNAIL/SLUG exhibited strong and variable immunoreactivity in PLCs in contrast to weak or absent E-cadherin expression. SOX10 was diffusely and strongly positive. *PLAG1* rearrangement was present in 1 pMYO.

Conclusions. PLCs mostly fail to express myoepithelial markers; PLCs are neoplastic cells adapting to microenvironmental changes and capable of EMT; and tumors composed solely of PLCs are apparently SPAs depleted of a ductal component. (Oral Surg Oral Med Oral Pathol Oral Radiol 2019;128:515–529)

Plasmacytoid or hyaline cells (PLCs) in salivary pleomorphic adenoma (SPA) are well documented in the literature and regarded as modified myoepithelial cells. In infrequent cases where PLCs characterize the vast majority of[1] or the entire neoplastic parenchyma, as seen especially in minor salivary glands, the neoplasm has been defined as plasmacytoid myoepithelioma (pMYO).[2,3] However, ultrastructural,[4-8] histochemical,[9-11] and immunohistochemical[8,12,13] studies in PLCs have not confirmed frank evidence of a myoepithelial phenotype. Indeed, a few investigators have posited a ductal origin of these cells.[7,14,15]

PLCs are usually seen in association with a glycosaminoglycan-rich and, less often, hyalinized stroma. Interestingly, besides their classic appearance, PLCs may exhibit further phenotypic change, adopting a fusiform or even spindle shape, suggesting the possibility of epithelial–mesenchymal transition (EMT). The concept of EMT in SPA has not been given appropriate attention,[16] although such notion was raised many years ago under various descriptions and terminology.[17,18] The limited investigation of this hypothesis may be related to the perception that (1) nonluminal cells in SPA are neoplastic modified myoepithelia, the predominant cells in SPA; and (2) the myxochondroid, osseous, or collagenous stromal variations are their products.[19,20] Alternatively, EMT may elegantly explain the plasticity and dynamic transitions observed in the neoplastic cells of SPAs. If EMT is occurring, downregulation or upregulation of genes controlling the EMT process should be evident. Supporting this hypothesis, downregulation of E-cadherin[21] and upregulation of SNAIL/SLUG has been reported in adenoid cystic carcinoma.[22]

Given our hypothesis that PLCs are nonmyoepithelial cells capable of EMT, we had 3 goals in this

Statement of Clinical Relevance

Plasmacytoid cells in salivary pleomorphic adenoma and myoepithelioma fail to consistently express myoepithelial markers, whereas epithelial–mesenchymal transition may elegantly explain the plasticity and dynamic transitions observed in neoplastic cells in this group of salivary gland tumors.

[a]Division of Oral and Maxillofacial Pathology, School of Dentistry, University of Minnesota, Minneapolis, MN, USA.
[b]Department of Laboratory Medicine and Pathology, University of Minnesota Medical School, University of Minnesota, Minneapolis, MN, USA.
[c]Department of Pathology, University of Chicago, Chicago, IL, USA.
[d]Department of Biochemistry, Molecular Biology and Biophysics, College of Biological Sciences, University of Minnesota, Minneapolis, MN, USA.
Received for publication Nov 12, 2018; returned for revision Jan 2, 2019; accepted for publication Jan 29, 2019.

2212-4403/$-see front matter
https://doi.org/10.1016/j.oooo.2019.01.081

project: (1) to study the properties of PLCs with currently available and accepted or purported immunohistochemical markers of normal and neoplastic myoepithelium; (2) to investigate the expression of EMT markers by immunohistochemistry; and (3) to evaluate cases of pMYO for aberrations of *PLAG1* by fluorescence in situ hybridization (FISH), knowing that *PLAG1* rearrangements have been infrequently reported in myoepithelioma (MYO).[23,24]

MATERIALS AND METHODS

Specimen selection and tissue procurement

The present study was approved by the University of Minnesota Institutional Review Board (IRB #1406M51491). All cases studied were archived formalin-fixed, paraffin-embedded minor salivary gland tumor tissues. The cohort included 4 SPAs with PLC predominance, 4 SPAs with insignificant or no PLC component, and 3 pMYO. Tumors diagnosed as pMYOs had no or very few neoplastic ductal structures after multiple consecutive tissue sections.[3] Hematoxylin and eosin (H&E)−stained sections of all tumors were reviewed by 2 of us (I.G.K., P.P.A.) to confirm the diagnosis. The clinical information is summarized in Table I.

Immunohistochemical analysis of PLCs in minor salivary gland tumors

For the first part of the study, the immunoprofile of PLCs in SPAs and pMYO was investigated for the expression of several critical proteins: structural filamentous components K14 (myoepithelium) and K7 (myoepithelial and acinar/ductal cells), α-smooth muscle actin (α-SMA), calponin and h-caldesmon; p63/p40 (nuclear markers of normal myoepithelia); S100 (S100 protein, a nonspecific marker of neoplastic myoepithelium); and, D2-40 and DOG1 (novel myoepithelial markers). For the second part of the study, we investigated EMT-related proteins SNAIL/SLUG, E-cadherin, WT1,[25] and SOX10,[26,27] which have also been reported to be myoepithelial markers. The immunophenotype of PLCs was analyzed in conjunction with the parenchymatous spindle cells of SPA because such a phenotype may represent a late stage of EMT. In addition to standard positive controls for all antibodies, normal minor salivary glands included in the tumors served as internal controls. All primary antibodies used in this study are tabulated in Table II.

Fluorescence in situ hybridization

FISH was performed on formalin-fixed, paraffin-embedded tissue specimens of pMYO by using a breakapart probe to *PLAG1*(8q12.1) (Empire Genomics, Buffalo, NY). Twenty-five to 50 cells were analyzed for each tumor studied; cells were interpreted as positive for rearrangement when at least 2 signal widths separated the 3' and 5' components of the probe. To validate the probe and to serve as additional positive and negative controls for *PLAG1* genetic aberrations, we also tested cases of SPA, epithelial−myoepithelial carcinoma, and carcinoma-ex SPA.

RESULTS

Immunohistochemical features of PLCs in pMYO and SPA

K7 and K14 expression was positive in normal ductal and myoepithelial cells. PLCs in pMYO (Figures 1A−1C) and SPA (Figures 1D−1F) exhibited strong and scattered to diffuse, membranous and cytoplasmic positivity for K7 and rare focal K14 positivity (see Figures 1A−1F), whereas the spindle cell population of SPA appeared, overall, K7- and K14-negative (Figures 1G−1I).

Normal myoepithelia were positive for α-SMA, calponin, and h-caldesmon. The vast majority of PLCs were negative for α-SMA (Figures 2A and 2F) and uniformly negative for h-caldesmon (Figures 2B and 2G). Rare α-SMA-positive cells were observed at the

Table I. Presentation of the clinicopathologic characteristics and *PLAG1* rearrangement status of the minor salivary gland neoplasms with prominent PLC component analyzed in this study

Case No.	*Age/Sex*	*Location*	*Histopathologic diagnosis*	*PLAG1 rearrangement status*
1	42/M	Hard palate	PLC-rich SPA	Positive
2	26/F	Hard palate	PLC-rich SPA	Hybridization failed
3	21/F	Hard palate	PLC-rich SPA	Positive
4	81/M	Hard palate	PLC-rich SPA	Hybridization failed
5	56/M	Hard palate	SPA	Positive
6	48/F	Upper lip	SPA	Positive
7	39/F	Soft palate	SPA	Positive
8	15/M	Upper lip	SPA	Negative
9	35/F	Maxillary vestibule	pMYO	Negative
10	93/F	Maxillary vestibule	pMYO	Positive
11	53/M	Hard palate	pMYO	Negative

PLC, plasmacytoid cells; *pMYO,* plasmacytoid myoepithelioma; *PLAG1*, pleomorphic adenoma gene 1; *SPA,* salivary pleomorphic adenoma.

Table II. Collective presentation of the primary antibodies used for the immunohistochemical analysis of plasmacytoid cells (PLCs) in benign salivary gland tumors

Primary antibody	*Clone*	*Source*	*Dilution*	*Incubation time (min)*	*Antigen retrieval method*
anti-α-SMA	1A4, mouse monoclonal	Cell Marque	1:400	32	No antigen retrieval
anti-calponin	CALP, mouse monoclonal	DAKO	1:50	60	Steamer, citrate Buffer 20 minutes
anti-p63	4A4, mouse monoclonal	Biocare Medical	1:50	60	Steamer, citrate Buffer 20 minutes
anti-p40	BC28, mouse monoclonal	Ventana	1:200	16	CC1 for 32 minutes
anti-CK7	OV-TL 12/30, mouse monoclonal	DAKO	1:50	60	Steamer, Tris-EDTA pH 9, 20 minutes
anti-WT-1	6F-H2, mouse monoclonal	DAKO	1:50	60	Proteinase K, 5 minutes
anti-S100	4C4.9, mouse monoclonal	Thermo Fisher	1:100	60	Steamer, citrate Buffer 20 minutes
anti-SOX10	Rabbit polyclonal	Cell Marque	1:100	60	Epitope retrieval 2, 20 min Bond RX
anti-D2-40	D2-40, mouse monoclonal	DAKO	1:50	32	CC1 for 60 minutes
anti-h-caldesmon	h-isoform of caldesmon	DAKO	predilute	32	Standard CC1 for 64 minutes
anti-DOG1	SP31	Cell Marque	predilute	32	Standard CC1 for 64 minutes
anti-CK14	LL002	Biocare Medical	1:100	30	Steamer, Diva Decloaker, 20 minutes
anti-SNAIL/SLUG	Rabbit polyclonal	Abcam	1:100	Overnight	Steamer, Tris-EDTA pH 9, 60 minutes
anti-E-cadherin	H-108, Rabbit polyclonal	Santa-Cruz	1:100	Overnight	Steamer, Tris-EDTA pH 9, 60 minutes

α-SMA, α-smooth muscle actin; *WT1,* Wilms tumor 1; *CC1,* cell conditioning 1.

periphery of the PLC tumor nests and in proximity to tumor stroma (see Figure 2F). Calponin staining in PLCs varied from absent or weakly positive to moderate and diffuse (Figures 2C and 2H). Spindle cells in SPA exhibited strong and diffuse expression of α-SMA (Figure 2K) and calponin (Figure 2M) and weak or negative staining for h-caldesmon (Figure 2L).

Nuclei of normal myoepithelia were decorated with p63/p40. With the exception of a few isolated cells, staining for p63/p40 was negative in pMYO PLCs (Figures 2D and 2E). However, in PLC-rich SPA, random and selective p63/p40 nuclear immunoreactivity was observed (Figure 2I and 2J). In contrast, selective p63/p40 positivity was observed in the spindle cells of SPA (Figures 2N and 2O).

S100 staining was positive in some ductal cells and equivocal for normal myoepithelium. PLCs showed strong and diffuse, nuclear and cytoplasmic S100 immunoreactivity (Figures 3A and 3D). The vast majority of luminal cells of neoplastic ducts in SPAs were negative. DOG1 was negative in normal salivary glands. DOG1 was consistently and uniformly negative in PLCs (Figures 3B and 3E). D2-40 was positive in normal myoepithelia. PLCs in pMYO and PLC-rich

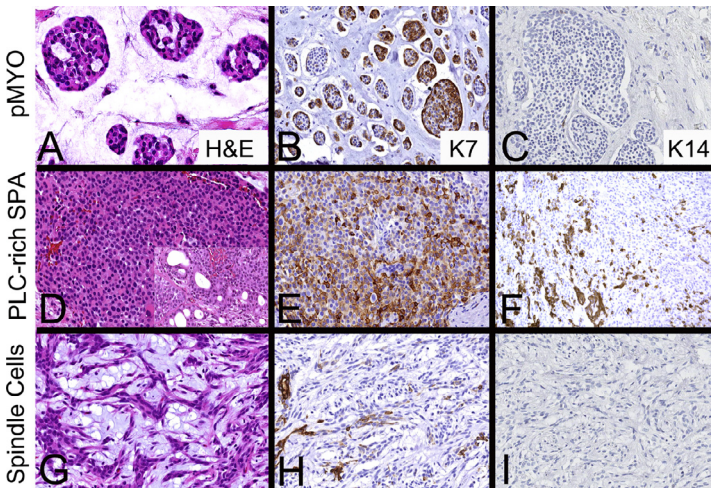

Fig. 1. **(A), (D), (G),** The microscopic features of plasmacytoid cells (PLCs) in plasmacytoid myoepithelioma (pMYO) and PLC-rich salivary pleomorphic adenoma (SPA) (the inset demonstrates typical bilayered ducts in a different area of the same tumor), and the spindle cells in SPA. **(B), (E), (H),** Keratin 7 (K7). **(C), (F), (I),** Keratin 14 (K14). PLCs in pMYO and SPA exhibited strong and scattered to diffuse, membranous and cytoplasmic positivity for K7 and rare focal K14 positivity. Spindle cells in SPA were, overall, K7- and K14-negative (hematoxylin ad eosin [H&E] and immunoperoxidase stain; original magnification A, D, and G: × 320; B, C, E, F, H, and I: × 270).

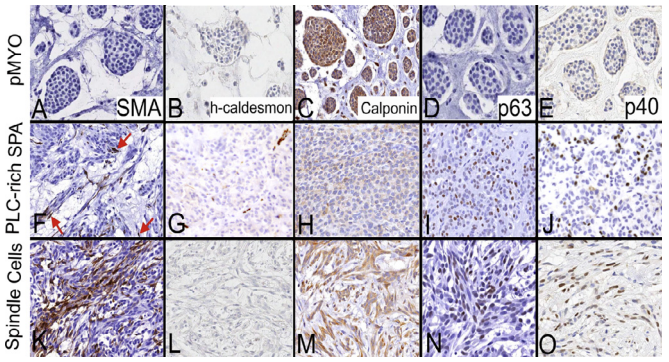

Fig. 2. **(A), (F), (K),** α-Smooth muscle actin (SMA). The vast majority of plasmacytoid cells (PLCs) were negative for α-SMA. Red arrows indicate apparent epithelial−mesenchymal transition of α-SMA negative plasmacytoid cells (PLCs) into α-SMA−-positive fusiform and spindle cells at the periphery of the tumor nests adjacent to the stroma. Spindle cells in salivary pleomorphic adenoma (SPA) exhibited strong and diffuse expression of α-SMA. **(B), (G), (L),** h-caldesmon. PLCs were uniformly negative for h-caldesmon, whereas spindle cells showed weak or negative staining. **(C), (H), (M),** Calponin. Calponin staining in PLCs varied from absent or weakly positive to moderate and diffuse. Spindle cells in SPA exhibited strong and diffuse expression of calponin. **(D), (I), (N),** p63. **(E), (J), (O),** p40. Staining for p63/p40 was, overall, negative in plasmacytoid myoepithelioma (pMYO) PLCs. However, in PLC-rich SPA, random and selective p63/p40 nuclear immunoreactivity was observed. Selective p63/p40 positivity was observed in spindle cells of SPA (immunoperoxidase stain; original magnification A−O: × 340).

SPA exhibited selective and in areas diffuse, D2-40 cytoplasmic and membranous immunoreactivity, which tended to be stronger at the periphery of PLC nests and in proximity to the neoplastic stroma (Figures 3C and 3F). The spindle cell population in SPA was diffusely positive for S100 and D2-40 (Figures 3G and 3I), and negative for DOG1 (Figure 3H).

EMT-related markers in neoplastic cells revealed the following staining properties; WT1, which was not expressed in normal myoepithelia, was scattered to diffuse and moderate to strong in PLCs (Figures 4A and 4E). Interestingly, similar to D2-40, WT1 immunoreaction was stronger in some cases at the periphery of PLC tumor nests (see Figure 4E). SOX10 was positive in many, but not all, normal luminal and abluminal cells of intercalated ducts and serous acini and negative in mucous cells. PLCs exhibited strong and diffuse SOX10 nuclear immunostaining (Figures 4B and 4F). SNAIL/SLUG were positive in ductal cells and exhibited strong and variable, nuclear and cytoplasmic

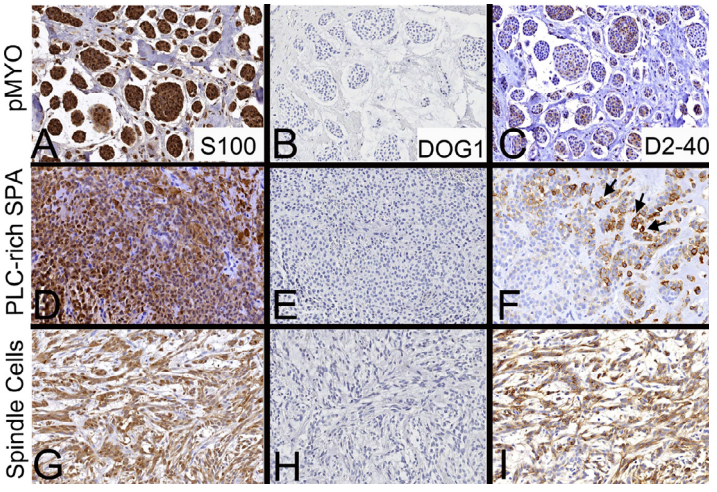

Fig. 3. (**A), (D), (G),** S100. Plasmacytoid cells (PLCs) and spindle cells showed strong and diffuse, nuclear and cytoplasmic S100 immunoreactivity. (**B), (E), (H),** DOG1. DOG1 was consistently and uniformly negative in PLCs and spindle cells. (**C), (F), (I),** D2-40. PLCs in plasmacytoid myoepithelioma (pMYO) and PLC-rich salivary pleomorphic adenoma (SPA) exhibited selective and in areas diffuse, D2-40 cytoplasmic and membranous immunoreactivity. Black arrows highlight increased D2-40 immunoreactivity at the periphery of PLC nests and in proximity to the neoplastic stroma. The spindle cell population in SPA was diffusely positive for D2-40 (immunoperoxidase stain; original magnification A−C: × 240; D−F: × 320, G−I: × 270).

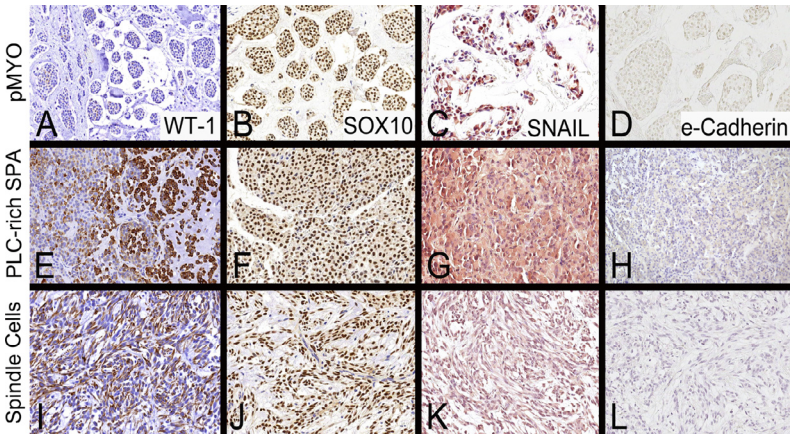

Fig. 4. **(A), (E), (I),** WT1. WT1 staining was scattered to diffuse and moderate to strong in plasmacytoid cells (PLCs). WT1 immunoreaction was stronger at the periphery of PLC tumor nests. The spindle cell population in SPA was diffusely positive for WT1. **(B), (F), (J),** SOX10. PLCs and spindle cells exhibited strong and diffuse SOX10 nuclear immunostaining. **(C), (G), (K),** SNAIL/SLUG. SNAIL/SLUG exhibited strong and variable, nuclear and cytoplasmic immunoreactivity in PLCs and diffuse positivity in spindle cells. **(D), (H), (L),** E-cadherin. E-cadherin expression was weak or absent in PLCs in plasmacytoid myoepithelioma (pMYO) and PLC-rich salivary pleomorphic adenoma (SPA), and negative in spindle cells in SPA (immunoperoxidase stain; original magnification A−D: × 240; E−L: × 270).

immunoreactivity in PLCs (Figures 4C and 4G) in contrast to weak or absent E-cadherin expression of the same areas (Figures 4D and 4H). The spindle cell population in SPA was diffusely positive for WT1 (Figure 4I), SOX10 (Figure 4J), and SNAIL/SLUG (Figure 4K), but negative for E-cadherin (Figure 4L).

PLAG1 rearrangement status in pMYO

One of the three pMYOs (Figures 5A−5D) and 5 of 6 successfully hybridized SPAs (Figures 6A−6D) exhibited *PLAG1* rearrangement. *PLAG1* rearrangement was observed in the apparent SPA component of carcinoma ex-SPA (Figures 7A and 7B), whereas epithelial−myoepithelial carcinoma was negative. The *PLAG1* rearrangement findings are summarized in Table I.

DISCUSSION

All epithelial components of salivary glands—acinar, ductal, and myoepithelial cells—have the capacity for proliferation[28-30] and, thus, can undergo neoplastic transformation. This has led to the postulate that in SPA, the neoplastic acinar−ductal unit, with modified myoepithelial cells being the predominant component, gives rise to the various parenchymatous and stromal types observed.[19,20] The significance of the myoepithelium has been emphasized by some authors who primarily compared the neoplastic parenchyma of SPA to adenomyoepithelioma of the breast,[31,32] supported by findings from histochemical studies.[31,33-35] However, these theories have not been universally accepted.[36,37]

PLCs have been typically included among the so-called modified myoepithelial cells. Ultrastructural studies of PLCs[4-6,8] have interpreted haphazardly arranged cytoplasmic fibrillar meshworks, composed of approximately 6-nm long intermediate fibrils as myofilamentous, despite the lack of dark bodies that represent aggregates of myofilaments in normal smooth muscle. The presence of these filaments, together with the fact that PLCs are neoplastic cells and, as such, are capable of phenotypic modifications, have been the reason for referring to them as modified neoplastic myoepithelia.[38] However, this theory has been challenged,[39] with Chaudhry et al.[7] and Ogawa

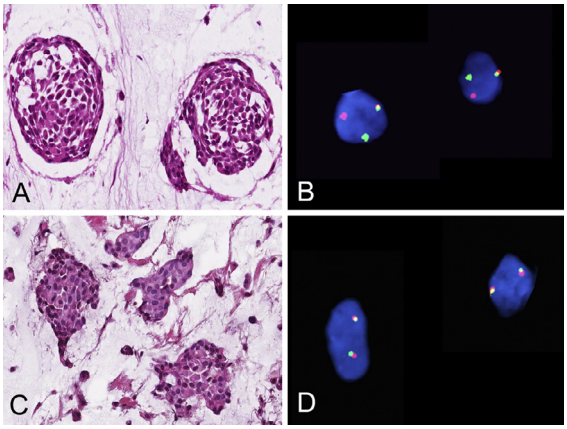

Fig. 5. **(A), (B),** This plasmacytoid myoepithelioma (pMYO) featured whorl-like aggregates of neoplastic cells with plasmacytoid morphology embedded in a rich myxoid stroma and was positive for *PLAG1* rearrangement (hematoxylin and eosin [H&E]; original magnification × 450). **(C), (D),** A case of pMYO with 2 intact copies of *PLAG1* in each cell (H&E; original magnification × 450).

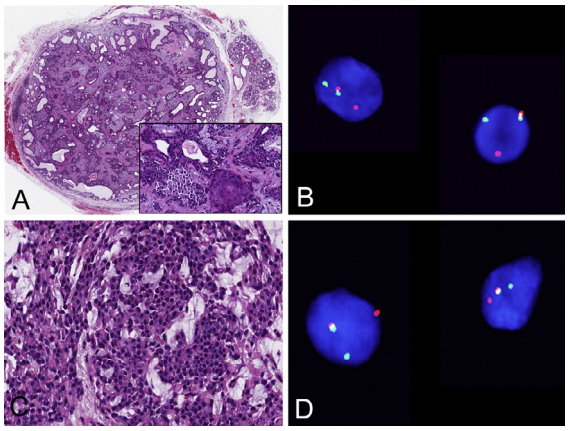

Fig. 6. **(A),** Histopathologic features of salivary pleomorphic adenoma (SPA). **(A)** A well-demarcated unencapsulated mass composed of neoplastic cells forming bilayered ductal structures (hematoxylin and eosin [H&E]; original magnification × 160; inset × 320). **(B),** Fluorescence in situ hybridization (FISH) analysis of the same case. This SPA exhibited *PLAG1* rearrangement, as confirmed by the 1 yellow (physiologic) signal and 2 separated green and red signals. **(C),** Microscopic characteristics of an example of plasmacytoid cell (PLC)−rich SPA. In different areas of the same specimen, ductal formation was noticed (H&E; original magnification × 450). **(D),** On FISH, this SPA with abundant PLCs showed *PLAG1* rearrangement.

et al.[15] stating that the origin of PLCs could be traced back to ductal cells.

Histochemical stains identifying normal myoepithelial cells have shown consistent staining of PLCs with tannic acid−phosphomolybdic acid−Levanol-fast cyanine 5RN, or azophloxine, amidoblack, and acid blue.[9,10] However, such stains have not been restricted to myoepithelia because positivity has also been observed in other cell types and structures, including the dental cuticle,[40] hyaline bodies in the wall of the odontogenic cysts,[41] and tonofilaments of the spinous layer of stratified squamous epithelium.[11]

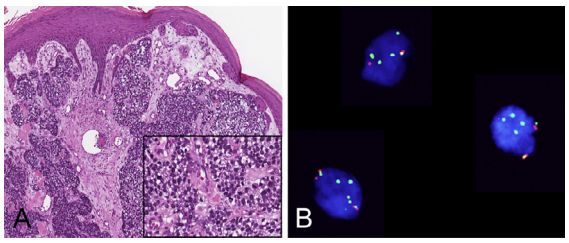

Fig. 7. **(A), (B),** Histopathologic and cytogenetic characteristics of the carcinoma ex-salivary pleomorphic adenoma (SPA). Islands and nests of malignant neoplastic cells with cytologic atypia and increased number of mitotic figures (see inset) diffusely infiltrating the fibrous connective tissue stroma (hematoxylin and eosin [H&E]; original magnification × 90; inset × 550). This case was *PLAG1* rearranged, as shown by the separated green and red signals.

PLC staining with α-SMA and h-caldesmon has been generally negative[8,12,13] and variable with K14[15,42,43] and calponin.[13,44,45] Calponin has been considered the most sensitive marker for the identification of neoplastic myoepithelium.[45] As such, staining of PLCs with an antibody targeting this intermediate filament can be regarded as confirmatory of a myoepithelial phenotype. However, Ogawa et al.[15] observed calponin positivity also in the ductal cells of normal salivary ducts and SPA. On the basis of that observation, they proposed a ductal origin not only for PLCs but also for other types of nonluminal cells. PLCs are apparently not unique to SPA because they have been reported in polymorphous (low-grade) adenocarcinoma[46] and even cutaneous basal cell carcinoma.[47] In the latter, their presence has been interpreted as myoepithelial differentiation of neoplastic basal cells.

Besides their classic appearance, PLCs may display spindled features in areas of discohesive cell aggregates, which occur, generally, in a glycosaminoglycan-rich stroma. This variation—taking into consideration that similar individual cell separation, "fraying out" (as depicted in Pierre Masson's *Human Tumors Histology, Diagnosis and Technique,* Figure 3.17 and Color Plate IV; Figure 2)[48] and spindling can be seen in the nonluminal cells of the ductal units in SPA—raises the possibility that EMT is the underlying mechanism of such process. EMT is not discussed in the classic articles by Dardick et al.[19,20] on the histogenesis of SPA, most likely because of lack of knowledge of the concept at that time and, certainly, of the EMT-related pathways. Specifically, the pioneering work of Elizabeth D. Hay[49,50] on EMT (*epithelial−mesenchymal transformation* was the term used then) took place in the middle 1980s, although Trelstad, Hay, and Revel[51] introduced the concept in 1967 while studying gastrulation in the chick embryo. EMT represents a process by which epithelial cells lose intercellular junctions and polarity and acquire migratory and invasive characteristics. EMT is critical for the development of numerous organs and tissues during embryogenesis and plays a role in gastrulation, neural crest formation, wound healing, and cancer progression.[52] It is possible that the detailed ultrastructural findings in Dardick's studies highlight structural changes suggestive or consistent with EMT, given our present knowledge on the subject. As discussed below, further support of EMT in SPA can be provided by expression or repression of genes regulating the EMT process.

The phenomenon or mechanism of EMT has been previously reported in the SPA literature, albeit with different descriptive terms. For example, Quintarelli and Robinson[18] suggested a mechanism of

"mesenchymalization," which may now meet the definition of EMT to explain cartilage formation in the stroma of SPA, a capability that has now been proven inherent in normal human submandibular gland cells that express chondrogenesis-related transcription factors SOX5, 6, and 9.[53] Harrison and Auger[17] used the term "stromalization" to describe the changes observed in the parenchyma of SPA, which, with apparent derepression of certain genes, result in the variations observed in the stroma of SPA.

Subsequently, German pathologists theorized that EMT is the mechanism responsible for the morphologic heterogeneity observed in the parenchyma and stroma of SPA[54,55] by identifying real mesenchymal phenotypes (e.g., collagen types II, III, and VI).[55] Staining of cell adhesion molecules, such as the neural cell adhesion molecules that participate in EMT during embryogenesis,[56] are positive on luminal cells with gradual loss of staining in nonluminal cells,[57] a pattern also observed with E-cadherin,[58,59] which is known to be downregulated in EMT. More recently, the notion of EMT is supported not only in SPA[16] but also in adenoid cystic carcinoma.[60]

In our hypothesis, we have challenged the theory that PLCs are modified myoepithelia and attempted to provide supporting evidence for their EMT capabilities. We repeated immunohistochemical staining with antibodies previously used to characterize PLCs to obtain a comprehensive picture of the properties of PLCs in each tumor studied. In most published articles, a myoepithelial phenotype of not only the PLCs but also the majority of tumor cells in SPA is accepted a priori. On that basis, attempts are made to fit results of the expression of various immunohistochemical markers in the model which postulates that the essential cell in SPA is the modified myoepithelium.[19,20]

Keratins

Immunohistochemical staining of normal myoepithelial cells with various keratins (e.g., K14, K17, and K19), has served as the basis for designating those keratins as indicative of a neoplastic myoepithelial phenotype. The mere fact that neighboring phenotypically similar cells may not stain at all can be puzzling, although expectation for all-or-nothing staining, when addressing immunohistochemical results in neoplasms, may be an overzealous axiomatic approach. The fact is, however, that such keratin stains are not specific for only normal myoepithelial cells because other structural elements of normal salivary glands, generally ducts, can be stained. Similarly, luminal cells in SPA can give positive staining.[16,44] In that manner, K14 positive staining can be seen in the ductal cells in the mucous glands of the palate[44] and the so-called basal cells of excretory ducts.[43] The staining of normal myoepithelia with K14 has been regarded as indicative of the binding of normal myoepithelial cells to the surrounding basement membrane of glands[61] and negative staining in PLCs is the result of absence of basement membrane.[61] de Araújo et al.[43] have reported rare positive staining of PLCs, and Ogawa et al.[15] staining in 6 of 12 cases studied, with generally less than 30% of PLCs decorated. Khurram and Speight[42] showed, focally, weak positive staining for K14, but generally negative staining.

K7, present in simple epithelia, stains myoepithelial cells weakly[62] or not at all[43], whereas ductal and, to a lesser extent, acinar cells can be decorated.[63] In our study, PLCs exhibited selective positive staining. Although luminal cells were positive for K7, spindle cells in SPA were rarely stained. In previous immunohistochemical analyses,[43,64] K7 stained PLCs, although the staining was not consistent. On the basis of our findings and the limited literature, it appears that PLCs tend to be positive for K7.

K19 can also stain normal myoepithelia[65] as well as ductal cells.[15] PLCs express K19 in greater than 50% of the cell population, which, together with K14 positivity and negativity for smooth muscle markers, led Ogawa et al.[15] to favor a nonmyoepithelial ductal phenotype for PLCs. Structural changes occurring in cells to adapt in the tumor microenvironment may better explain the variations seen in keratins.[16]

Smooth muscle markers

Microfilament proteins α-SMA and calponin have been traditionally and frequently used in the study of normal and neoplastic myoepithelial cells, instead of smooth muscle myosin and h-caldesmon. Among these markers, calponin has been considered superior,[42,45] although staining has been reported to be variable in all types of purported neoplastic myoepithelial cells. The absence of α-SMA in PLCs led Franquemont and Mills[12] to dispute their myoepithelial origin. Other studies have also confirmed negative or almost negative α-SMA immunostaining.[8,13,15,66] However, spindle cells in SPA and the so-called spindle cell MYO have been stained invariably with α-SMA; α-SMA is a key molecule in EMT.

Calponin and caldesmon are smooth muscle contraction regulatory proteins, with both binding to actin and calmodulin. Clones 1A4 (CALP [basic calponin]) and h-isoform of caldesmon are generally used in routine immunohistochemistry. On the basis of the literature and our results, one can argue that positive but variable staining with calponin should support the myoepithelial origin of PLCs. However, the CALP clone can also react with epithelial keratinocytes and nerves[14] because keratinocytes and nerves possess h2- and acidic calponins,

which show a high degree of homology to CALP. Calponin staining has been also observed in luminal cells,[13,44] suggesting possible cross-reaction with h2 and acidic calponin isoforms that are present in tonofilaments, which are abundant in PLCs.

Other markers of normal and neoplastic myoepithelia

S100

S100, which is negative in normal myoepithelium,[67] has been regarded as a neoplastic myoepithelial marker, although the specificity is considered low. S100 comprises a multigenic family of Ca^{+2}-binding proteins consisting of 24 subtypes that regulate intracellular Ca^{+2} and Ca^{+2} signaling pathways. S100 participates in a variety of cellular activities, including regulation of proliferation, differentiation, apoptosis, metabolism, migration/invasion, and inflammation. The clone used for the present work, 4C4.9, has affinity for S100A1 and S100B. Subtype S100A1 has been identified in the granular convoluted tubule and striated duct cells of the murine submandibular gland,[68] and both S100A1 and S100B have been observed in serous but not mucous acinar cells and intercalated duct cells.[69] It has been found that both ductal and myoepithelial cells in SPA contain DNA encoding S100B.[70] Binding partners of S100B are tubulin and the microtubule-associated protein, caldesmon, calponin, type III intermediate filament subunits and annexin 6.[71] S100B also regulates calcium homeostasis, which is essential in the functioning of salivary glands.[72] It is well-established that nonluminal cells are responsible for the secretion of glycosaminoglycans in the stroma.[17] S100 staining in salivary gland tumors may indicate that S100 participates in intercellular and intracellular signal transduction, energy metabolism, contraction, and cell growth.[73,74] Alternatively, the presence of S100 may compensate for the apparent lack of or minimal innervation and neuroeffector relationships in salivary gland tumors, including SPA.[75]

DOG-1

The exocrine secretory process of normal salivary gland acini involves regulation of intracellular and extracellular calcium. This is coordinated by Ca^{2+}-activated chloride channel (CaCC) currents at the apical (luminal) portions of individual acinar cells. Differences in chloride kinetics among major salivary glands have been shown to be related to their differences in function.[76] The genes responsible for the CaCC are *TME16A&B* (renamed *ANO1&2*) and *anoctamin1&2*). *TME16A (ANO1)* is known to bench pathologists as *DOG-1 (Discovered on GIST1)* because of its consistent high expression in gastrointestinal stromal tissues. In normal salivary glands, variable apical staining with DOG-1 is reported in the serous acini of the parotid and, to a lesser degree, in the distal portions of intercalated ducts and mucous acini. Staining of acinic cell carcinoma was confirmed by Chênevert et al.[77] DOG-1 utility as an important antibody differentiating acinic cell carcinoma from other salivary gland tumors has been established,[77] especially when the classic basophilic granular presentation is limited or lacking. A good example is the differentiation of acinic cell carcinoma from the so-called secretory carcinoma variant of the acinic cell/intercalated family of tumors.[78] According to Chênevert et al.,[77] neoplastic myoepithelial cells are stained in adenoid cystic carcinoma and epithelial−myoepithelial carcinoma, but not in MYO, SPA, and most of myoepithelial carcinomas. Khurram and Speight[42] reported some "myoepithelial staining" in SPA but not in MYO. Interestingly, the same investigators reported more frequent focal luminal cell staining in SPAs, suggesting a similar staining profile with intercalated ducts. On the basis of that observation, possible recapitulation of the secretory activity of intercalated ducts was suggested. Generally, secretory activity of neoplastic lumina is deficient compared with that of normal ducts.[17] It is our opinion that DOG-1 should not be utilized as a myoepithelial marker because it does not stain normal myoepithelium; if it is used, however, it should be with caution, similar to WT1 (see below). Negative staining may simply indicate the absence of CaCCs from neoplastic cells, whereas positive staining may highlight retention of such channels that may relate to focal acidification of the glycoproteinaceous intraluminal secretion.

p63/p40

The *TP53*-related transcription factor p63 participates in epithelial commitment, differentiation, and maintenance of integrity, both during embryologic development and in adult tissues by means of its regulation of greater than 80 genes that directly control its over- or underexpression.[79] Six different isoforms of p63 exist as a result of alternative splicing at the C-terminus and the presence or absence of an N-terminal transactivation domain (TA). The absence of the N-terminal TA is designated as ΔNp63 isoform. The role of p63 in epithelial proliferation is substantial and maintained in the basal and suprabasal cell layers by blocking apoptosis via inhibition of p21.[80] Overexpression of ΔNp63 upregulates cell adhesion.[81] Overexpression of ΔNp63 upregulates cell adhesion,[81] loss of p63 leads to lack of differentiation and cell cycle arrest, and mutations cause ectrodactyly, ectodermal dysplasia, and clefting-related conditions, as well as limb mammary syndrome, acro-onicho-lacrimal-dental syndrome, and split hand/foot malformations.[82] For purposes of differentiation and integrity, p63 directly induces *IKKα, Jagged1*,[83] and a number of cell-to-cell and cell-to-matrix adhesion factors[84], while simultaneously suppressing mesodermal induction.

The utility of p63 in surgical pathology is broad. The ΔNp63 isoform is detected by the commercially available antibody p40, whereas the p63 antibody (clone 4A4) recognizes both ΔNp63 and TAp63 isoforms. For example, both p63 and p40 antibodies stain the nuclei of the basal and suprabasal cell layers of the oral mucosal epithelium and not the upper differentiated keratin layers. This finding can be clearly demonstrated even in odontogenic cysts.[85] Concordant, nondiscriminatory p63/p40 staining is observed in odontogenic tumors.[85]

Nuclear immunoreactivity for p63/p40 is observed in the normal myoepithelia of breast and salivary glands, and p63 staining in salivary gland tumors has been regarded as confirmatory of a basal/myoepithelial cell phenotype. Recently, p40 has been favored as a more specific marker of normal and neoplastic myoepithelium.[86,87] The presence or absence of p40 immunoreactivity has been used for algorithmic differential diagnosis in cases of adenoid cystic carcinoma and polymorphous (low-grade) adenocarcinoma, especially in small biopsy material.[87,88]

In SPA[87] and pMYO, immunohistochemical evidence of nuclear p63/p40 positivity has been variable, and an attempt to classify parenchymatous cells as modified or transformed myoepithelia may lead to confusion. In the present study, p63/p40 staining was generally negative in the PLCs in pMYO. However, in some cases of PLC-rich SPA, selective p63/p40 nuclear immunoreactivity was observed. The possibility that these markers identify other functional characteristics and not merely a basal/myoepithelial phenotype has been raised.[88] Loss of p63 prevents expression of K14.[89] Given the multitude of p63 isoforms function, one can thus theorize that in SPA p63/p40−positive nonluminal cells may show cell-to-cell and cell-to-matrix interactions, whereas p63/p40−negative ductal structures represent terminally differentiated neoplastic cells.

The role of p63 isoforms in EMT is well-documented.[90,91] In cancer progression, downregulation of ΔNp63 leads to repression of Wnt and induction of a mesenchymal phenotype.[83,90] In addition, inhibiting ΔNp63 upregulates the genes that promote mesenchymal morphology and motility, such as N-cadherin.[91] On the basis of the above findings, loss of ΔNp63 expression in PLCs, confirmed by p40 immunonegativity, may indicate EMT attributes. In our opinion, considering p63/p40 as simply a myoepithelial phenotypic marker overlooks many of the properties of p63 and its participation in tumor development and progression.[83]

D2-40

Podoplanin (D2-40) is a transmembrane mucin glycoprotein initially identified in the renal podocytes responsible for the maintenance of their foot processes and glomerular permeability.[92] Podoplanin, which is expressed in type I cells of the rat lung and in lymphatic development, is essential for development; *Podoplanin*−/− phenotype is lethal in mice because of respiratory and lymphatic defects.[93]

Podoplanin affinity for lymphatic, but not vascular, endothelial cells has been utilized as a discriminatory immunohistochemical marker for lymphatic endothelium. However, podoplanin is also expressed in a variety of other tissues, including the basal and suprabasal cells of stratified epithelia[94]; the inner and outer epithelia of the cervical loop of the developing tooth at the bell stage; the odontoblastic cell layer, but not the other cells of the dental papilla, osteocytes, and osteoblasts[95]; mesothelial cells[96]; follicular dendritic cells[97]; fetal germ cells and developing Sertoli cells[98]; and tumors deriving from some of the cell types above (e.g., squamous cell carcinoma, germ cell tumors, and epithelioid mesotheliomas).

In mice, podoplanin is strongly expressed in the basal portion of the intercalated, striated, and terminal ducts of major salivary glands, in acinar and ductal myoepithelial cells, in mucous cells, and, to a lesser degree, in the basal portion of the serous acinar units of the major salivary glands.[99] The molecular structure of podoplanin is resistant to proteases because of its mucinous glycoproteinaceous property and the high sialic acid content, thus providing protection to acinar units.[100] In myoepithelial cells, podoplanin promotes plasma membrane extension and actin cytoskeleton rearrangement.[99] This is achieved through directly binding to phosphorylated ezrin, a participant in EMT, as the result of direct activation of *RHOA*, a RAS homologue gene family member A (RhoA) guanosine triphosphatase, and *ROCK1*, a Rho-associated protein kinase.[101] However, actin rearrangement may be also accomplished independent of RhoA and, as such, without E-cadherin downregulation and ezrin upregulation.[102]

In SPA, in accordance with our findings, podoplanin immunostaining has been identified in the various types of neoplastic cells, including PLCs and spindle cells, but not the luminal cells.[103] No difference was noted between the D2-40 staining patterns of PLCs in SPA and pMYO. We also observed an increase in staining intensity of PLCs in the periphery of some neoplastic islands, as well as in smaller nests and cords of PLCs in direct association with the tumor stroma.

Of interest is the reported co-localization and interaction of podoplanin and CD44, a hyaluronic acid receptor to promote cell motility in skin tumorigenesis.[104] Given that CD44 is expressed in the parenchymal cells of SPA,[105] increased levels of D2-40 may lead to increased CD44 recruitment at the cell membrane, cellular migration, and, finally, the acquisition of an EMT-permissive phenotype.

Markers of EMT

SNAIL/SLUG and E-cadherin

SNAI1, also referred to as *SNAIL*, and *SNAI2,* which is commonly known as *SLUG,* are pivotal regulators of EMT.[106] Both *SNAIL* and *SLUG* belong to the snail C2H2-type zinc-finger protein family of transcription factors. *SNAIL,* which is localized to both cytoplasm and nucleus, depending on its phosphorylation status,[107] is involved in the formation and maintenance of embryonic mesoderm and is expressed in a variety of human tissues, especially the kidney. In contrast, *SLUG,* which is typically localized to the nucleus, participates in the migration of neural crest cells and is expressed in abundance in the placenta and in the adult heart, pancreas, liver, kidneys, and skeletal muscle.[106]

Several lines of evidence suggest that *SNAIL/SLUG*−mediated EMT has a central role in carcinogenesis through enhancement of migration, invasiveness, and metastatic dissemination in various human tumors.[106,108] The mechanism by which *SNAIL/SLUG* drive the acquisition of mesenchymal cellular features is well-documented: *SNAIL* represses E-cadherin expression, thus decreasing cell-to-cell adhesion, and transcriptionally upregulates N-cadherin ("cadherin switch") to induce EMT[109,110] in breast, ovarian, endometrial, hepatocellular, thyroid, and head and neck malignancies.[111]

The expression levels and roles of *SNAIL* and *SLUG* have been thoroughly investigated in salivary adenoid cystic carcinoma, in which strong positive SNAIL and SLUG immunoreactivity is observed in approximately 60%[111] and 72%[112] of cases, respectively. Notably, SLUG protein expression is weaker in normal salivary glands and SPA compared with that in adenoid cystic carcinoma.[22] SNAIL/SLUG expression positively correlates with perineural invasion, local regional recurrence, and distant metastasis in patients with adenoid cystic carcinoma[111,112] Furthermore, SNAIL is required for epidermal growth factor−induced EMT in adenoid cystic carcinoma cell lines,[113] whereas *SLUG* silencing appears to inhibit EMT by restoring E-cadherin levels.[114] In this study, we observed that PLCs in the majority of salivary gland pMYO and SPA express the EMT-regulatory proteins SNAIL/SLUG, whereas expression of E-cadherin is entirely negative in accordance with previous findings.[21] Similarly, spindled neoplastic cells in SPA exhibit primarily nuclear and, to a lesser extent, cytoplasmic SNAIL/SLUG positivity.

WT1

WT1 is important in human development and a promoter of EMT. $WT1^{-/-}$ mice die in the middle of gestation as a result of disturbances in heart development, complete absence of kidneys and gonads, and various malformations affecting the liver, spleen, retina, and adrenal glands.[115] WT1 directly activates *SNAIL* and represses E-cadherin, thus promoting epicardial EMT and the generation of the heart vasculature.[115]

WT1 is not present in the normal components of salivary glands, including normal myoepithelial cells.[16,25] Langman et al.[25] have regarded WT1 as a superior myoepithelial marker over more established ones, such as calponin and p63. In our study, WT1 staining was observed in PLCs and in the spindle cell population of SPA in accordance with previous reports.[16,25] It should be noted here that immunohistochemical stains, absent in normal cells but present in neoplastic cells, should be interpreted with caution as indicative of specific cell type.[116] However, it is possible that WT1-positive cells in SPA and pMYO represent neoplastic myoepithelium because (1) although *WT1* is a tumor suppressor gene, it may exert oncogenic function because of epigenetic changes (i.e., promoter methylation);[117] and (2) activation of WT1 has been reported in solid tumors originating from tissues that do not express WT1 during embryonic development or in adulthood.[118]

Although nuclear WT1 staining should be expected, the observed cytoplasmic staining is apparently the result of post-translational phosphorylation and is not nonspecific or the result of antibody cross-reactivity with cytoplasmic elements.[25,118]

SOX10

SOX10, a member of the conserved *Sry* (sex-determining region Y)−related homeobox (Sox) transcription factor family, participates in embryonic, neural crest, and peripheral nervous system development.[119] As such, it has been utilized as a marker for melanoma and tumors of neural crest origin. Nuclear staining of SOX10 has been observed in the myoepithelial cells of the salivary, bronchial, and mammary glands.[120] However, in a study by Ohtomo et al.,[26] positive nuclear staining was also encountered in the acinar cells and both the luminal and nonluminal cells of the intercalated ducts of the normal major salivary glands in humans. Similar expression is observed during the developmental stages of murine acinar, luminal, and nonluminal cells of intercalated ducts.[26]

Notwithstanding the variations in expression, greater than 90% of PLCs have been reported to be SOX10 positive.[26] Additionally, some cases of cutaneous MYO and mixed tumors show staining in the majority of both luminal and abluminal cells.[27] Our experience is essentially the same as that in previous studies; PLCs in pMYO and spindle cells in SPA consistently show diffuse nuclear SOX10 immunostaining. The stain distribution of SOX10 in normal salivary glands does not support its discriminatory use as a neoplastic myoepithelial marker; thus, an acinar or intercalated duct origin for PLCs cannot be refuted and may, instead, be more plausible.[26]

SOX10 is a participant in EMT. There is evidence of similarities between neural crest migration and tumor metastasis, given that in both biologic processes, transforming growth factor-β, bone morphogenetic protein, Wnt, and FGF/receptor tyrosine kinase pathways are active. Among the transcription factors of the Wnt/BMP/FGF is SOX10.[121] Although *SOX10* participates in EMT, its presence in acinic cell carcinoma, where EMT is not expected,[78] probably indicates serous acinar/intercalated duct origin. As noted in our study, serous, but not mucous, cells in normal glands show positive nuclear staining. This observation should be confirmed by other studies and suggests a topic of future research.

PLAG1

Cytogenetic and molecular characteristics defining SPA have been well documented.[122-124] SPAs have been shown to harbor specific chromosomal aberrations, resulting in the formation of chimeric fusion genes involving *PLAG1* and, infrequently, *HMGA2* (12q14-15).[24,122,123,125-127] *PLAG1* fusion partners include *CTNNB1, CHCHD7, LIFR*, and *TCEA1*,[24,123,128,129] and *HMGA2* fusion partners include *NFIB, FHIT*, and *WIFI*.[124,130,131] We focused on *PLAG1* rearrangement in this study because *PLAG1* chromosomal rearrangements and/or fusion transcripts have been identified in up to 88% of SPA.[24] Supporting a genetic link between MYO and SPA, El-Naggar et al.[23] reported a MYO of the parotid gland characterized by aberrations involving the long arm of chromosome 12, and in the study by Martins et al.,[24] a MYO was found to be rearranged for *PLAG1*. In our study, 1 of 3 pMYO featured *PLAG1* rearrangement. The absence of *PLAG1* rearrangement in pMYO may indicate aberrations of other genes, including *HMGA2*.

CONCLUSIONS

Our goal in this study was to investigate the dynamic behavior of PLCs and, to some extent, of other parenchymal cells in SPA "as the key to the understanding of their development and function."[132] On the basis of our findings, and in conjunction with the results of previous studies, we came to the following conclusions:

1. PLCs mostly fail to consistently express myoepithelial markers.
2. PLCs represent neoplastic cells that have adapted to changes in their microenvironment and are capable of EMT.
3. Tumors composed solely of PLCs are SPAs depleted of a ductal component; thus, instead of the term *pMYO*, we favor the term *plasmacytoid predominant SPA*. The term *plasmacytoid adenoma* may also be appropriate.[12]
4. The current World Health Organization definition of SPA may be improved by incorporating the terminology by Triantafyllou et al.[16]—"a benign epithelial tumor that is characterized by variable EMT, secretion/differentiation, and metaplasia."

It is important to note that EMT and neoplastic myoepithelial cells are not mutually exclusive because a myoepithelial phenotype can result from EMT. In the near future, new markers will undoubtedly be reported as being specific for myoepithelial cells in SPA and other salivary gland tumors. We hope that such markers are viewed and interpreted in the context of their corresponding gene function, rather than simply used to identify a postulated phenotype.

PRESENTATION

Parts of this study were presented at the 2016 AAOMP Annual Meeting in San Diego, CA, USA, and at the 2017 USCAP Annual Meeting in San Antonio, TX, USA.

ACKNOWLEDGMENTS

We would like to thank Dr. Elizabeth A. Bilodeau, School of Dental Medicine, University of Pittsburgh, Pittsburg, PA, for her valuable assistance in this project; and Mr. Brian Dunnette, University of Minnesota, Minneapolis, MN, for his assistance with the preparation of the illustrations.

REFERENCES

1. Dardick I, Thomas MJ, van Nostrand AW. Myoepithelioma—new concepts of histology and classification: a light and electron microscopic study. *Ultrastruct Pathol*. 1989;13:187-224.
2. El-Naggar AK, Chan JKC, Grandis JR, Takata T, PJ S. Tumors of salivary glands. In: *WHO Classification of Head and Neck Tumours*. 4 Lyon, France: International Agency for Research on Cancer (IARC); 2017:159-201.
3. Ellis GL, Auclair PL. Benign epithelial neoplasms: myoepithelioma. In: *Tumors of the Salivary Glands. AFIP Atlas of Tumor Pathology*. Fourth Series, Fascicle 9. Washington, DC: ARP; 2008:123-133.
4. Kahn LB, Schoub L. Myoepithelioma of the palate. Histochemical and ultrastructural observations. *Arch Pathol*. 1973;95:209-212.
5. Lomax-Smith JD, Azzopardi JG. The hyaline cell: a distinctive feature of "mixed" salivary tumours. *Histopathology*. 1978;2:77-92.
6. Sciubba JJ, Brannon RB. Myoepithelioma of salivary glands: report of 23 cases. *Cancer*. 1982;49:562-572.
7. Chaudhry AP, Labay GR, Yamane GM, Jacobs MS, Cutler LS, Watkins KV. Clinico-pathologic and histogenetic study of 189 intraoral minor salivary gland tumors. *J Oral Med*. 1984;39:58-78.
8. Dardick I, Cavell S, Boivin M, et al. Salivary gland myoepithelioma variants. Histological, ultrastructural, and immunocytological features. *Virchows Arch A Pathol Anat Histopathol*. 1989;416:25-42.
9. Nikai H, el-Bardaie AM, Takata T, Ogawa I, Ijuhin N. Histologic evaluation of myoepithelial participation in salivary gland tumors. *Int J Oral Maxillofac Surg*. 1986;15:597-605.

10. Triantafyllou AG. Histochemical detection of myoepithelial cells in pleomorphic adenoma with azophloxine and amidoblack. *J Oral Med*. 1986;41:184-188.
11. Triantafyllou A. Histochemical study of hyaline cells of pleomorphic adenoma with azophloxin, amidoblack and acid blue. *Arch Pathol Anat*. 1988;2:31-38. [in Greek].
12. Franquemont DW, Mills SE. Plasmacytoid monomorphic adenoma of salivary glands. Absence of myogenous differentiation and comparison to spindle cell myoepithelioma. *Am J Surg Pathol*. 1993;17:146-153.
13. Furuse C, Sousa SO, Nunes FD, Magalhães MH, Araújo VC. Myoepithelial cell markers in salivary gland neoplasms. *Int J Surg Pathol*. 2005;13:57-65.
14. Ogawa Y. Immunocytochemistry of myoepithelial cells in the salivary glands. *Prog Histochem Cytochem*. 2003;38:343-426.
15. Ogawa Y, Kishino M, Atsumi Y, et al. Plasmacytoid cells in salivary-gland pleomorphic adenomas: evidence of luminal cell differentiation. *Virchows Arch*. 2003;443:625-634.
16. Triantafyllou A, Thompson LD, Devaney KO, et al. Functional histology of salivary gland pleomorphic adenoma: an appraisal. *Head Neck Pathol*. 2015;9:387-404.
17. Harrison JD, Auger DW. Mucosubstance histochemistry of pleomorphic adenoma of parotid and submandibular salivary glands of man: light and electron microscopy. *Histochem J*. 1991;23:293-302.
18. Quintarelli G, Robinson L. The glycosaminoglycans of salivary gland tumors: a histochemical characterization and a critical evaluation. *Am J Pathol*. 1967;51:19-37.
19. Dardick I, van Nostrand AW, Jeans MT, Rippstein P, Edwards V. Pleomorphic adenoma, I: ultrastructural organization of "epithelial" regions. *Hum Pathol*. 1983;14:780-797.
20. Dardick I, Van Nostrand AW, Jeans MT, Rippstein P, Edwards V. Pleomorphic adenoma, II: ultrastructural organization of "stromal" regions. *Hum Pathol*. 1983;14:798-809.
21. Economopoulou P, Hanby A, Odell EW. Expression of E-cadherin, cellular differentiation and polarity in epithelial salivary neoplasms. *Oral Oncol*. 2000;36:515-518.
22. Bu LL, Deng WW, Huang CF, Liu B, Zhang WF, Sun ZJ. Inhibition of STAT3 reduces proliferation and invasion in salivary gland adenoid cystic carcinoma. *Am J Cancer Res*. 2015;5:1751-1761.
23. el-Naggar AK, Lovell M, Callender DL, Ordonez NG, Killary AM. Cytogenetic analysis of a primary salivary gland myoepithelioma. *Cancer Genet Cytogenet*. 1999;113:49-53.
24. Martins C, Fonseca I, Roque L, et al. *PLAG1* gene alterations in salivary gland pleomorphic adenoma and carcinoma ex-pleomorphic adenoma: a combined study using chromosome banding, *in situ* hybridization and immunocytochemistry. *Mod Pathol*. 2005;18:1048-1055.
25. Langman G, Andrews CL, Weissferdt A. WT1 expression in salivary gland pleomorphic adenomas: a reliable marker of the neoplastic myoepithelium. *Mod Pathol*. 2011;24:168-174.
26. Ohtomo R, Mori T, Shibata S, et al. SOX10 is a novel marker of acinus and intercalated duct differentiation in salivary gland tumors: a clue to the histogenesis for tumor diagnosis. *Mod Pathol*. 2013;26:1041-1050.
27. Naujokas A, Charli-Joseph Y, Ruben BS, et al. SOX-10 expression in cutaneous myoepitheliomas and mixed tumors. *J Cutan Pathol*. 2014;41:353-363.
28. Barka T. Stimulation of DNA synthesis by isoproterenol in the salivary gland. *Exp Cell Res*. 1965;39:355-364.
29. Walker NI, Gobé GC. Cell death and cell proliferation during atrophy of the rat parotid gland induced by duct obstruction. *J Pathol*. 1987;153:333-344.
30. Dardick I, Byard RW, Carnegie JA. A review of the proliferative capacity of major salivary glands and the relationship to current concepts of neoplasia in salivary glands. *Oral Surg Oral Med Oral Pathol*. 1990;69:53-67.
31. Bauer WH, Bauer JD. Classification of glandular tumors of salivary glands: study of one-hundred forty-three cases. *AMA Arch Pathol*. 1953;55:328-346.
32. Günther R. Myoepitheliale wucherungen in der brustdrüse. *Virchows Arch Path Anat*. 1937;300:449-455.
33. Azzopardi JG, Smith OD. Salivary gland tumours and their mucins. *J Pathol Bacteriol*. 1959;77:131-140.
34. Mylius EA. The identification and the role of the myoepithelial cell in salivary gland tumours. *Acta Pathol Microbiol Scand Suppl*. 1960;50:1-81.
35. Grishman E. Histochemical analysis of mucopolysaccharides occurring in mucus-producing tumors: mixed tumors of the parotid gland, colloid carcinomas of the breast, and myxomas. *Cancer*. 1952;5:700-707.
36. Palmer RM, Lucas RB, Knight J, Gusterson B. Immunocytochemical identification of cell types in pleomorphic adenoma, with particular reference to myoepithelial cells. *J Pathol*. 1985;146:213-220.
37. Palmer RM, Lucas RB, Langdon JD. Ultrastructural analysis of salivary gland pleomorphic adenoma, with particular reference to myoepithelial cells. *Histopathology*. 1985;9:1061-1076.
38. Dardick I. Myoepithelioma: definitions and diagnostic criteria. *Ultrastruct Pathol*. 1995;19:335-345.
39. Harris M. Hyaline cells in mixed salivary neoplasms. *Histopathology*. 1979;3:248-249.
40. Hodson JJ. Origin and nature of the cuticula dentis. *Nature*. 1966;209:990-993.
41. Sedano HO, Gorlin RJ. Hyaline bodies of Rushton. Some histochemical considerations concerning their etiology. *Oral Surg Oral Med Oral Pathol*. 1968;26:198-201.
42. Khurram SA, Speight PM. Characterisation of DOG-1 expression in salivary gland tumours and comparison with myoepithelial markers. *Head Neck Pathol*. 2018 Apr 18. https://doi.org/10.1007/s12105-018-0917-3. [Epub ahead of print].
43. de Araújo VC, de Sousa SO. Expression of different keratins in salivary gland tumours. *Eur J Cancer B Oral Oncol*. 1996;32B:14-18.
44. Ogawa Y, Toyosawa S, Ishida T, Ijuhin N. Keratin 14 immunoreactive cells in pleomorphic adenomas and adenoid cystic carcinomas of salivary glands. *Virchows Arch*. 2000;437:58-68.
45. Savera AT, Gown AM, Zarbo RJ. Immunolocalization of three novel smooth muscle-specific proteins in salivary gland pleomorphic adenoma: assessment of the morphogenetic role of myoepithelium. *Mod Pathol*. 1997;10:1093-1100.
46. Dos Santos HT, de Andrade BA, Egal ES, Filho ER, Mariano FV, Altemani A. Plasmacytoid-type cellular differentiation in polymorphous low-grade adenocarcinoma. *Int J Surg Pathol*. 2016;24:322-327.
47. Cohen PR. Basal cell carcinoma with myoepithelial differentiation: case report and literature review. *Cureus*. 2018;10:e2081.
48. Masson P. *Human Tumors Histology, Diagnosis and Technique* [translated by SD Kobernick]. ed. 2. Detroit, MI: Wayne State University Press; 1970.
49. Greenburg G, Hay ED. Epithelia suspended in collagen gels can lose polarity and express characteristics of migrating mesenchymal cells. *J Cell Biol*. 1982;95:333-339.
50. Hay ED. An overview of epithelio-mesenchymal transformation. *Acta Anat (Basel)*. 1995;154:8-20.
51. Trelstad RL, Hay ED, Revel JD. Cell contact during early morphogenesis in the chick embryo. *Dev Biol*. 1967;16:78-106.
52. Thiery JP, Acloque H, Huang RY, Nieto MA. Epithelial-mesenchymal transitions in development and disease. *Cell*. 2009;139:871-890.

53. Matsumoto Y, Sato S, Maeda T, et al. Transcription factors related to chondrogenesis in pleomorphic adenoma of the salivary gland: a mechanism of mesenchymal tissue formation. *Lab Invest*. 2016;96:16-24.
54. Aigner T, Neureiter D, Völker U, Belke J, Kirchner T. Epithelial-mesenchymal transdifferentiation and extracellular matrix gene expression in pleomorphic adenomas of the parotid salivary gland. *J Pathol*. 1998;186:178-185.
55. Neureiter D, Böhmer J, Kirchner T, Aigner T. Pleomorphic adenomas of the parotid express different mesenchymal phenotypes: demonstration of matrix gene expression products characteristic of the fibroblastic and chondrocytic cell lineages. *Histopathology*. 1999;35:373-379.
56. Cunningham B, Edelman G. Structure, expression, and cell surface modulation of cell adhesion molecules. In: Edelman GM, Cunningham BA, Thiery JP, eds. *Morphoregulatory Molecules*, New York: Wiley; 1990:9-40.
57. Saleh ER, França CM, Marques MM. Neural adhesion molecule (N-CAM) in pleomorphic adenoma and carcinoma ex-pleomorphic adenoma. *J Oral Pathol Med*. 2003;32:562-567.
58. Enescu A, Enescu A, Florou C, Petrescu F. E-cadherin and α-SMA expression in the epithelial-mesenchymal transition of salivary glands pleomorphic adenomas. *Rom J Morphol Embryol*. 2014;55:1383-1387.
59. Prabhu S, Kaveri H, Rekha K. Benign, malignant salivary gland tumors: comparison of immunohistochemical expression of E-cadherin. *Oral Oncol*. 2009;45:594-599.
60. Ma SR, Mao L, Deng WW, et al. AGR2 promotes the proliferation, migration and regulates epithelial-mesenchymal transition in salivary adenoid cystic carcinoma. *Am J Transl Res*. 2017;9:507-519.
61. Santos EP, Cavalcante DR, Melo AU, Pereira JC, Gomes MZ, Albuquerque RL. Plasmacytoid myoepithelioma of minor salivary glands: report of case with emphasis in the immunohistochemical findings. *Head Face Med*. 2011;7:24.
62. Zhu S, Schuerch C, Hunt J. Review and updates of immunohistochemistry in selected salivary gland and head and neck tumors. *Arch Pathol Lab Med*. 2015;139:55-66.
63. Draeger A, Nathrath WB, Lane EB, Sundström BE, Stigbrand TI. Cytokeratins, smooth muscle actin and vimentin in human normal salivary gland and pleomorphic adenomas. Immunohistochemical studies with particular reference to myoepithelial and basal cells. *APMIS*. 1991;99:405-415.
64. Argyris PP, Gopalakrishnan R, Pambuccian SE, Tosios KI, Koutlas IG. Polymorphous low-grade adenocarcinoma of the upper lip with metachronous myoepithelioma of the buccal mucosa. *Oral Surg Oral Med Oral Pathol Oral Radiol*. 2014;117:e441-e448.
65. Triantafyllou A, Hunt JL, Devaney KO, Ferlito A. A perspective of comparative salivary and breast pathology. Part I: Microstructural aspects, adaptations and cellular events. *Eur Arch Otorhinolaryngol*. 2014;271:647-663.
66. Souliou CE, Tzermpos F, Argyris P, Tosios K. Plasmacytoid myoepithelioma of the hard palate: case report. *Acta Stomatol Croat*. 2017;51:152-156.
67. Dardick I, Stratis M, Parks WR, DeNardi FG, Kahn HJ. S-100 protein antibodies do not label normal salivary gland myoepithelium. Histogenetic implications for salivary gland tumors. *Am J Pathol*. 1991;138:619-628.
68. Mori M, Yamada K, Ohomura H, et al. Immunohistochemical localization of S100A1 and S100A6 in postnatally developing salivary glands of rats. *Histochem Cell Biol*. 1998;110:579-587.
69. Barrett AW, Scully C. S100 protein in oral biology and pathology. *J Oral Pathol Med*. 1994;23:433-440.
70. Landry CF, Kahn HJ, Baumal R, Marks A, Brown IR. Heterogeneity in expression of S100 beta mRNA in human melanoma and pleomorphic adenoma demonstrated by in situ hybridization. *Am J Pathol*. 1991;139:1151-1156.
71. Donato R. S100: a multigenic family of calcium-modulated proteins of the EF-hand type with intracellular and extracellular functional roles. *Int J Biochem Cell Biol*. 2001;33:637-668.
72. Homann V, Kinne-Saffran E, Arnold WH, Gaengler P, Kinne RK. Calcium transport in human salivary glands: a proposed model of calcium secretion into saliva. *Histochem Cell Biol*. 2006;125:583-591.
73. Zimmer DB, Cornwall EH, Landar A, Song W. The S100 protein family: history, function, and expression. *Brain Res Bull*. 1995;37:417-429.
74. Heizmann CW, Fritz G, Schäfer BW. S100 proteins: structure, functions and pathology. *Front Biosci*. 2002;7:d1356-d1368.
75. Triantafyllou A, Coulter P, Scott J. Phenotypes in canalicular adenoma of human minor salivary glands reflect the interplay of altered secretory product, absent neuro-effector relationships and the diversity of the microenvironment. *Histopathology*. 1999;35:502-516.
76. Kondo Y, Nakamoto T, Jaramillo Y, Choi S, Catalan MA, Melvin JE. Functional differences in the acinar cells of the murine major salivary glands. *J Dent Res*. 2015;94:715-721.
77. Chênevert J, Duvvuri U, Chiosea S, et al. DOG1: a novel marker of salivary acinar and intercalated duct differentiation. *Mod Pathol*. 2012;25:919-929.
78. Vander Poorten V, Triantafyllou A, Thompson LD, et al. Salivary acinic cell carcinoma: reappraisal and update. *Eur Arch Otorhinolaryngol*. 2016;273:3511-3531.
79. Perez CA, Pietenpol JA. Transcriptional programs regulated by p63 in normal epithelium and tumors. *Cell Cycle*. 2007;6:246-254.
80. Truong AB, Khavari PA. Control of keratinocyte proliferation and differentiation by p63. *Cell Cycle*. 2007;6:295-299.
81. Trink B, Osada M, Ratovitski E, Sidransky D. p63 transcriptional regulation of epithelial integrity and cancer. *Cell Cycle*. 2007;6:240-245.
82. Brunner HG, Hamel BC, Van Bokhoven H. The p63 gene in EEC and other syndromes. *J Med Genet*. 2002;39:377-381.
83. Talos F, Schulz R, Moll UM. p63 and canonical Wnt signaling. *Cell Cycle*. 2010;9:648-649.
84. Carroll DK, Brugge JS, Attardi LD. p63, cell adhesion and survival. *Cell Cycle*. 2007;6:255-261.
85. Argyris PP, Malz C, Taleb R, Koutlas IG. Benign and malignant odontogenic neoplasms of the jaws show a concordant nondiscriminatory p63/p40 positive immunophenotype. *Oral Surg Oral Med Oral Pathol Oral Radiol*. 2018;126:506-512.
86. Bishop JA, Teruya-Feldstein J, Westra WH, Pelosi G, Travis WD, Rekhtman N. p40 (ΔNp63) is superior to p63 for the diagnosis of pulmonary squamous cell carcinoma. *Mod Pathol*. 2012;25:405-415.
87. Rooper L, Sharma R, Bishop JA. Polymorphous low grade adenocarcinoma has a consistent p63+/p40- immunophenotype that helps distinguish it from adenoid cystic carcinoma and cellular pleomorphic adenoma. *Head Neck Pathol*. 2015;9:79-84.
88. Argyris PP, Wetzel SL, Greipp P, et al. Clinical utility of myb rearrangement detection and p63/p40 immunophenotyping in the diagnosis of adenoid cystic carcinoma of minor salivary glands: a pilot study. *Oral Surg Oral Med Oral Pathol Oral Radiol*. 2016;121:282-289.
89. Mills AA, Zheng B, Wang XJ, Vogel H, Roop DR, Bradley A. p63 is a p53 homologue required for limb and epidermal morphogenesis. *Nature*. 1999;398:708-713.
90. Drewelus I, Göpfert C, Hippel C, et al. p63 antagonizes Wnt-induced transcription. *Cell Cycle*. 2010;9:580-587.

91. Stacy AJ, Craig MP, Sakaram S, Kadakia M. ΔNp63α and microRNAs: leveraging the epithelial-mesenchymal transition. *Oncotarget*. 2017;8:2114-2129.
92. Breiteneder-Geleff S, Soleiman A, Horvat R, Amann G, Kowalski H, Kerjaschki D. Podoplanin—a specific marker for lymphatic endothelium expressed in angiosarcoma. *Verh Dtsch Ges Pathol*. 1999;83:270-275. [in German].
93. Schacht V, Ramirez MI, Hong YK, et al. T1alpha/podoplanin deficiency disrupts normal lymphatic vasculature formation and causes lymphedema. *EMBO J*. 2003;22:3546-3556.
94. Kawaguchi H, El-Naggar AK, Papadimitrakopoulou V, et al. Podoplanin: a novel marker for oral cancer risk in patients with oral premalignancy. *J Clin Oncol*. 2008;26:354-360.
95. Sawa Y, Iwasawa K, Ishikawa H. Expression of podoplanin in the mouse tooth germ and apical bud cells. *Acta Histochem Cytochem*. 2008;41:121-126.
96. Chu AY, Litzky LA, Pasha TL, Acs G, Zhang PJ. Utility of D2-40, a novel mesothelial marker, in the diagnosis of malignant mesothelioma. *Mod Pathol*. 2005;18:105-110.
97. Yu H, Gibson JA, Pinkus GS, Hornick JL. Podoplanin (D2-40) is a novel marker for follicular dendritic cell tumors. *Am J Clin Pathol*. 2007;128:776-782.
98. Yu H, Pinkus GS, Hornick JL. Diffuse membranous immunoreactivity for podoplanin (D2-40) distinguishes primary and metastatic seminomas from other germ cell tumors and metastatic neoplasms. *Am J Clin Pathol*. 2007;128:767-775.
99. Hata M, Ueki T, Sato A, Kojima H, Sawa Y. Expression of podoplanin in the mouse salivary glands. *Arch Oral Biol*. 2008;53:835-841.
100. Suzuki-Inoue K, Kato Y, Inoue O, et al. Involvement of the snake toxin receptor CLEC-2, in podoplanin-mediated platelet activation, by cancer cells. *J Biol Chem*. 2007;282:25993-26001.
101. Martín-Villar E, Megías D, Castel S, Yurrita MM, Vilaró S, Quintanilla M. Podoplanin binds ERM proteins to activate RhoA and promote epithelial-mesenchymal transition. *J Cell Sci*. 2006;119:4541-4553.
102. Wicki A, Lehembre F, Wick N, Hantusch B, Kerjaschki D, Christofori G. Tumor invasion in the absence of epithelial-mesenchymal transition: podoplanin-mediated remodeling of the actin cytoskeleton. *Cancer Cell*. 2006;9:261-272.
103. Tsuneki M, Maruyama S, Yamazaki M, et al. Podoplanin is a novel myoepithelial cell marker in pleomorphic adenoma and other salivary gland tumors with myoepithelial differentiation. *Virchows Arch*. 2013;462:297-305.
104. Martín-Villar E, Fernández-Muñoz B, Parsons M, et al. Podoplanin associates with CD44 to promote directional cell migration. *Mol Biol Cell*. 2010;21:4387-4399.
105. Xing R, Regezi JA, Stern M, Shuster S, Stern R. Hyaluronan and CD44 expression in minor salivary gland tumors. *Oral Dis*. 1998;4:241-247.
106. Kalluri R, Weinberg RA. The basics of epithelial-mesenchymal transition. *J Clin Invest*. 2009;119:1420-1428.
107. Brabletz T, Kalluri R, Nieto MA, Weinberg RA. EMT in cancer. *Nat Rev Cancer*. 2018;18:128-134.
108. Thiery JP, Sleeman JP. Complex networks orchestrate epithelial-mesenchymal transitions. *Nat Rev Mol Cell Biol*. 2006;7:131-142.
109. Yokoyama K, Kamata N, Hayashi E, et al. Reverse correlation of E-cadherin and snail expression in oral squamous cell carcinoma cells in vitro. *Oral Oncol*. 2001;37:65-71.
110. Batlle E, Sancho E, Francí C, et al. The transcription factor snail is a repressor of E-cadherin gene expression in epithelial tumour cells. *Nat Cell Biol*. 2000;2:84-89.
111. Jiang J, Tang Y, Zhu G, Zheng M, Yang J, Liang X. Correlation between transcription factor Snail1 expression and prognosis in adenoid cystic carcinoma of salivary gland. *Oral Surg Oral Med Oral Pathol Oral Radiol Endod*. 2010;110:764-769.
112. Tang Y, Liang X, Zheng M, et al. Expression of c-kit and Slug correlates with invasion and metastasis of salivary adenoid cystic carcinoma. *Oral Oncol*. 2010;46:311-316.
113. Wang Y, Hu J, Ye W, et al. EGFR activation induced Snail-dependent EMT and myc-dependent PD-L1 in human salivary adenoid cystic carcinoma cells. *Cell Cycle*. 2018:1-14.
114. Wu B, Wei J, Hu Z, et al. Slug silencing inhibited perineural invasion through regulation of EMMPRIN expression in human salivary adenoid cystic carcinoma. *Tumour Biol*. 2016;37:2161-2169.
115. Martínez-Estrada OM, Lettice LA, Essafi A, et al. Wt1 is required for cardiovascular progenitor cell formation through transcriptional control of Snail and E-cadherin. *Nat Genet*. 2010;42:89-93.
116. Leader R, Deol-Poonia RK, Sheard J, Triantafyllou A. Immunohistochemical localization of WT1 in epithelial salivary tumors. *Pathol Res Pract*. 2014;210:726-732.
117. Loeb DM, Sukumar S. The role of WT1 in oncogenesis: tumor suppressor or oncogene? *Int J Hematol*. 2002;76:117-126.
118. Hohenstein P, Hastie ND. The many facets of the Wilms' tumour gene. *WT1*. *Hum Mol Genet*. 2006;15:R196-R201.
119. Huber WE, Price ER, Widlund HR, et al. A tissue-restricted cAMP transcriptional response: SOX10 modulates alpha-melanocyte-stimulating hormone-triggered expression of microphthalmia-associated transcription factor in melanocytes. *J Biol Chem*. 2003;278:45224-45230.
120. Nonaka D, Chiriboga L, Rubin BP. Sox10: a pan-schwannian and melanocytic marker. *Am J Surg Pathol*. 2008;32:1291-1298.
121. Theveneau E, Mayor R. Neural crest migration: interplay between chemorepellents, chemoattractants, contact inhibition, epithelial-mesenchymal transition, and collective cell migration. *Wiley Interdiscip Rev Dev Biol*. 2012;1:435-445.
122. Stenman G. Fusion oncogenes in salivary gland tumors: molecular and clinical consequences. *Head Neck Pathol*. 2013;7:S12-S19.
123. Kas K, Voz ML, Röijer E, et al. Promoter swapping between the genes for a novel zinc finger protein and beta-catenin in pleiomorphic adenomas with t(3;8)(p21;q12) translocations. *Nat Genet*. 1997;15:170-174.
124. Geurts JM, Schoenmakers EF, Röijer E, Aström AK, Stenman G, van de Ven WJ. Identification of *NFIB* as recurrent translocation partner gene of HMGIC in pleomorphic adenomas. *Oncogene*. 1998;16:865-872.
125. Bullerdiek J, Wobst G, Meyer-Bolte K, et al. Cytogenetic subtyping of 220 salivary gland pleomorphic adenomas: correlation to occurrence, histological subtype, and in vitro cellular behavior. *Cancer Genet Cytogenet*. 1993;65:27-31.
126. Mark J, Dahlenfors R, Wedell B. Impact of the in vitro technique used on the cytogenetic patterns in pleomorphic adenomas. *Cancer Genet Cytogenet*. 1997;95:9-15.

127. Weinreb I. Translocation-associated salivary gland tumors: a review and update. *Adv Anat Pathol*. 2013;20:367-377.
128. Aström AK, Voz ML, Kas K, et al. Conserved mechanism of PLAG1 activation in salivary gland tumors with and without chromosome 8q12 abnormalities: identification of SII as a new fusion partner gene. *Cancer Res*. 1999;59: 918-923.
129. Asp J, Persson F, Kost-Alimova M, Stenman G. CHCHD7-PLAG1 and TCEA1-PLAG1 gene fusions resulting from cryptic, intrachromosomal 8q rearrangements in pleomorphic salivary gland adenomas. *Genes Chromosomes Cancer*. 2006;45: 820-828.
130. Geurts JM, Schoenmakers EF, Van de Ven WJ. Molecular characterization of a complex chromosomal rearrangement in a pleomorphic salivary gland adenoma involving the 3'-UTR of HMGIC. *Cancer Genet Cytogenet*. 1997;95:198-205.
131. Persson F, Andrén Y, Winnes M, et al. High-resolution genomic profiling of adenomas and carcinomas of the salivary glands reveals amplification, rearrangement, and fusion of HMGA2. *Genes Chromosomes Cancer*. 2009;48:69-82.
132. Weiss P. The cell in development. *Lab Invest*. 1959;8:415-430.

Reprint requests:

Ioannis G. Koutlas,
Division of Oral and Maxillofacial Pathology,
School of Dentistry, University of Minnesota,
515 Delaware Street SE 16-116B,
Minneapolis,
MN 55455,
USA
Koutl001@umn.edu